6-2-2017

Trypanosoma brucei RAP1 Maintains Telomere and Subtelomere Integrity by Suppressing TERRA and Telomeric RNA: DNA Hybrids

Vishal Nanavaty
Cleveland State University

Ranjodh Sandhu
Cleveland State University

Sanaa E. Jehi
Cleveland State University

Unnati M. Pandya
Cleveland State University

Bibo Li
Cleveland State University, B.LI37@csuohio.edu

Published online 16 March 2017

Nucleic Acids Research, 2017, Vol. 45, No. 10 ***5785–5796***
doi: 10.1093/nar/gkx184

Trypanosoma brucei RAP1 maintains telomere and subtelomere integrity by suppressing TERRA and telomeric RNA:DNA hybrids

Vishal Nanavaty[1], Ranjodh Sandhu[1], Sanaa E. Jehi[1], Unnati M. Pandya[1] and Bibo Li[1,2,3,4,*]

[1]Center for Gene Regulation in Health and Disease, Department of Biological, Geological, and Environmental Sciences, Cleveland State University, 2121 Euclid Avenue, Cleveland, OH 44115, USA, [2]The Rockefeller University, 1230 York Avenue, New York, NY 10065, USA, [3]Department of Immunology, Lerner Research Institute, Cleveland Clinic, 9500 Euclid Avenue, Cleveland, OH 44195, USA and [4]Case Comprehensive Cancer Center, Case Western Reserve University, 10900 Euclid Avenue, Cleveland, OH 44106, USA

Received February 10, 2017; Editorial Decision March 06, 2017; Accepted March 08, 2017

ABSTRACT

Trypanosoma brucei **causes human African trypanosomiasis and regularly switches its major surface antigen, VSG, thereby evading the host's immune response. VSGs are monoallelically expressed from subtelomeric expression sites (ESs), and VSG switching exploits subtelomere plasticity. However, subtelomere integrity is essential for *T. brucei* viability. The telomeric transcript, TERRA, was detected in *T. brucei* previously. We now show that the active ES-adjacent telomere is transcribed. We find that *Tb*RAP1, a telomere protein essential for VSG silencing, suppresses *VSG* gene conversion-mediated switching. Importantly, *Tb*RAP1 depletion increases the TERRA level, which appears to result from longer read-through into the telomere downstream of the active ES. Depletion of *Tb*RAP1 also results in more telomeric RNA:DNA hybrids and more double strand breaks (DSBs) at telomeres and subtelomeres. In *Tb*RAP1-depleted cells, expression of excessive *Tb*RNaseH1, which cleaves the RNA strand of the RNA:DNA hybrid, brought telomeric RNA:DNA hybrids, telomeric/subtelomeric DSBs and VSG switching frequency back to WT levels. Therefore, *Tb*RAP1-regulated appropriate levels of TERRA and telomeric RNA:DNA hybrid are fundamental to subtelomere/telomere integrity. Our study revealed for the first time an important role of a long, non-coding RNA in antigenic variation and demonstrated a link between telomeric silencing and subtelomere/telomere integrity through *Tb*RAP1-regulated telomere transcription.**

INTRODUCTION

Subtelomeres are regions immediately upstream of telomeres at chromosome ends. The relatively plastic and fragile environment at subtelomeres allows more frequent DNA rearrangements (1) and facilitates gene conversion-mediated antigenic variation in microbial pathogens such as *Trypanosoma brucei* that causes human African trypanosomiasis, *Pneumocystis jerovecii* that causes pneumonia, and *Borrelia burgdorferi* that causes Lyme disease, as the major surface antigens are transcribed from subtelomeric expression sites in these pathogens (2). However, introduction of a single DNA double strand break (DSB) at certain subtelomeric loci results in lethality in >90% of *T. brucei* cells (3), underlying the importance of subtelomere integrity. Subtelomere integrity is also important for human health. Deletion of subtelomeric D4Z4 repeats derepresses a nearby *DUX4* gene in muscle cells and leads to facioscapulohumeral muscular dystrophy (4). 5% of unexplained human mental impairment cases are caused by cryptic unbalanced subtelomeric rearrangements (5). Additionally, olfactory receptor genes and immunoglobulin heavy chain genes are located at human subtelomeric regions (6).

Regular switching of the major surface antigen, VSG, is an important pathogenesis mechanism in *T. brucei*, which has >2500 complete and truncated *VSG* genes (7). VSGs are transcribed by RNA Polymerase I (RNAP I) (8) exclusively from one of 15 different subtelomeric expression sites (ESs) (9,10). Genes in *T. brucei* are arranged in polycistronic transcription units (PTUs), and ESs are typical PTUs with *VSG* being the last gene in any ES. Monoal-

*To whom correspondence should be addressed. Tel: +1 216 6872444; Fax: +1 216 6876972; Email: b.li37@csuohio.edu
Present addresses:
Ranjodh Sandhu, Department of Microbiology and Molecular Genetics, University of California Davis, One Shields Avenue, Davis, CA 95616, USA.
Sanaa E. Jehi, The Scripps Research Institute, Department of Molecular and Experimental Medicine, La Jolla, CA 92037, USA.
Unnati M. Pandya, Department of Medicine, Division of Translational Medicine, New York University School of Medicine, New York, NY, USA.

lelic VSG expression is regulated at multiple levels, including ES promoter activation and silencing, chromatin structure remodeling, and specialized subnuclear localization of the active ES [reviewed in (11)]. Additionally, ES attenuation (12) and the inositol phosphate pathway (13) also affect VSG silencing. Particularly, silent ES promoters are actually mildly active but transcription only elongates for a few kilobases along the PTU, preventing expression of downstream *VSGs* (14). Therefore, regulation of transcription elongation along ESs is important for VSG silencing. We have shown that *Tb*RAP1, a telomere protein, is essential for repressing subtelomeric *VSG* expression by telomeric silencing and have proposed that *Tb*RAP1 helps suppress transcription elongation along ESs (15,16).

VSG switching occurs through two major pathways (Supplementary Figure S1). In an *in situ* switch, the originally active ES is silenced while a different ES becomes expressed simultaneously. DNA recombination mediates the other major class of VSG switching. In crossover (CO)/telomere exchange (TE), the active *VSG* and a silent *VSG* (often with its downstream telomeric DNA) exchange places, resulting in the expression of a different VSG from the same active ES without losing any genetic information. In gene conversion (GC), a silent *VSG* gene is duplicated into the active ES to replace the originally active *VSG* gene, which is lost. Usually, the term 'VSG GC' is used when GC events encompass only the *VSG* gene and its neighboring sequences, while 'ES GC' refers to events that encompass most of the ES, sometimes including the ES promoter. A number of proteins important for DNA recombination, such as RAD51 (17), RAD51-3 (18), BRCA2 (19), RECQ2 (20), TOPO3α (21) and TOPO3α-interacting RMI1 (22) play important roles in VSG switching. In addition, we and others have shown that telomeres and telomere-associated proteins affect VSG switching (23–25).

Telomeres are essential for protecting the natural chromosome ends from being recognized as DNA breaks, and telomere proteins help prevent chromosome ends from being processed illegitimately (26). Recently, we showed that telomere proteins are also important for maintaining subtelomere integrity and stability (24,25,27). In addition, telomeres suppress expression of nearby genes by telomeric silencing (28). In yeasts, it is well accepted that the telomere heterochromatic structure limits the access of the transcription machinery to promoters of subtelomeric genes and silencing is at the transcription activation level rather than at the elongation step (28), while in *T. brucei*, we have proposed that the *Tb*RAP1-mediated telomeric silencing helps block transcription elongation (15), although the exact mechanism is unknown.

In many organisms including *T. brucei*, telomeres are transcribed into a long, non-coding telomeric repeat-containing RNA (TERRA), which contains G-rich telomeric sequences (29,30). TERRA is transcribed by RNA Polymerase II in mammalian cells and yeast (31,32), but its transcription is resistant to α-Amanitin in *T. brucei*, suggesting that it is transcribed by RNAP I (29). In *Saccharomyces cerevisiae*, TERRA expression and stability are regulated by the telomere-binding factor RAP1 (33). Recent studies showed that TERRA can form R-loops (a three-stranded structure including an RNA:DNA hybrid and a displaced single-stranded DNA) with the telomeric DNA in yeast and human cells, and a high level of telomeric R-loops promotes telomere recombination events (30). R-loops have been hypothesized to interfere with DNA replication, and R-loop-dependent replication impairment has been implicated in transcription-associated recombination (34). The R-loop structure can be resolved by RNaseH, which degrades the RNA moiety in the RNA:DNA hybrid (35). In telomerase-nagative tumor cells, RNaseH1-depleted cells have increased amount of RNA:DNA hybrids, while overexpression of RNaseH1 reduces the occurrence of telomeric R-loops (36). Whether *T. brucei* TERRA can form telomeric R-loops and influence nearby VSG switching is unknown.

In *T. brucei*, *Tb*TRF is the duplex telomere DNA binding factor (37), and it interacts with both *Tb*RAP1 (15) and *Tb*TIF2 (25). We have shown that all three telomere proteins are essential for cell viability, *Tb*RAP1 is essential for *VSG* silencing (15,16), and both *Tb*TRF and *Tb*TIF2 suppress VSG switching (24,25). However, it was not clear why *TbRAP1* is an essential gene and whether *Tb*RAP1 affects VSG switching and the expression of TERRA. By performing an *in vitro* VSG switching assay we found that a transient depletion of *Tb*RAP1 led to a higher VSG switching frequency with most switchers arising from VSG GC. In addition, TERRA and telomeric RNA:DNA hybrid levels were increased in *Tb*RAP1-depleted cells. Depletion of *Tb*RAP1 also led to more DSBs at telomeres and at ES-linked *VSG* loci. Importantly, expression of an ectopic allele of *Tb*RNaseH1 in *Tb*RAP1-depleted cells lowered the telomeric RNA:DNA hybrids, telomeric/subtelomeric DSBs, and VSG switching frequency back to WT levels. Therefore, depletion of *Tb*RAP1 increases TERRA and telomeric RNA:DNA hybrid levels, the latter of which facilitates DSB-initiated *VSG* gene conversion and subsequent VSG switching.

MATERIALS AND METHODS

Examination of telomeric RNA:DNA hybrid

One hundred microgram of genomic DNA was isolated from induced (+Dox for 24 h) and uninduced S/RAP1i and S/RAP1i+RNaseH1-2HA cells and sonicated with a BioRuptor (Diagenode) using medium output for eight cycles with 30 s pulse each. Half of the sonicated samples were treated with 20 U of RNaseH (Thermo Fisher Scientific). Both RNaseH treated and untreated samples were equally divided for IP using normal IgG or S9.6 antibodies. After extensive washing, the immunoprecipitated samples were eluted and loaded onto Nylon (+) membrane followed by Southern analysis using a TTAGGG repeat probe.

VSG switching assay, ligation-mediated PCR, cloning of the active VSG, and Pulsed-Field gel electrophoresis

These were performed exactly the same as described in (25). Additional details are described in Supplemental Information. Primers used for LMPCR are the same as those listed in (25).

Quantitative RT-PCR

Quantitative RT-PCR for estimation of VSG expression levels was performed the same way as in (15).

TERRA northern blotting and slot blot hybridization

Total RNA was purified from 100 million *T. brucei* cells using RNA STAT-60 (Tel. Test Inc.) twice and treated with 10 units of DNase I (Thermo Fisher Scientific) followed by another round of purification with RNA STAT-60. The resulting RNA sample was treated with or without 20 units of RNase One (Promega) and 20 μg of RNase A (Sigma) (as negative controls). For northern blotting, 10 μg of RNA samples were loaded in each lane. For slot blot hybridization, 2 μg of RNA was spotted on the Nylon membrane. RNA samples were denatured at 65°C for 10 min in the presence of formamide and formaldehyde before separated by electrophoresis. To prepare the $(CCCTAA)_n$- [or $(TTAGGG)_n$-] specific probe, the Klenow primer extension reaction was performed using a duplex TTAGGG repeats as the template in the presence of dA, dT and radioactive dC (or radioactive dG).

γH2A antibody production

A 10-amino acid peptide (CKHAKATPSV) from the C-terminus of *T. brucei* H2A was synthesized in two versions with the T residue either phosphorylated or not (ProSci), and the phosphorylated peptide was used to immunize two rabbits (ProSci). Both the phosphorylated and unphosphorylated peptides were coupled with SulfoLink Resin (Thermo Fisher Scientific) for affinity purification of the rabbit serum. Rabbit serum was first affinity purified through the column of unphosphorylated peptide to obtain antibodies recognizing the unphosphorylated H2A. The flow through fraction was subsequently affinity purified through the column with the phosphorylated peptide to obtain antibodies that specifically recognize γH2A.

RESULTS

*Tb*RAP1 suppresses VSG switching

We used the HSTB261 strain established by Kim and Cross (21) to examine the effects of *Tb*RAP1 depletion on VSG switching. HSTB261 (hereafter referred to as the S strain) has a *blasticidin resistance* (*BSD*) gene immediately downstream of the promoter and a *puromycin resistance* gene (*PUR*) fused with the *Herpes simplex Thymidine Kinase* (*TK*) gene between *VSG2* and 70 bp repeats in the active ES (Supplementary Figure S1) (21). We introduced the inducible *Tb*RAP1 RNAi construct into S cells to establish the S/RAP1i strain. *Tb*RAP1 is an essential protein, and depletion of *Tb*RAP1 leads to cell growth arrest within 24 h (15). Therefore, to recover viable switchers for estimation of switching frequency, we induced *Tb*RAP1 RNAi for only 24 h and removed doxycycline by extensive washing. This decreased *Tb*RAP1 protein levels (Figure 1A and B), slowed cell growth (Figure 1C), and derepressed ES-linked silent *VSGs* including *VSG13* and *VSG9* for ∼48 h (Figure 1B). Forty eight hours after removal of doxycycline, the *Tb*RAP1 protein and cell growth recovered to their normal levels (Figure 1A–C), and ES-linked *VSG9* and *VSG13* were silenced again (Figure 1B). Importantly, inducing *Tb*RAP1 RNAi by doxycycline in the recovered cells resulted in cell growth arrest again (Supplementary Figure S2A and B). Therefore, short-term depletion of *Tb*RAP1 is completely reversible. As controls, we examined *Tb*RAP1 protein levels in uninduced S/RAP1i cells (Supplementary Figure S2C) and in S (Figure 1A) and S/ev cells (S cells carrying an empty RNAi vector; Supplementary Figure S2D) in the presence of doxycycline. The *Tb*RAP1 protein level in these cells did not change.

We next performed the VSG switching assay. All cells were grown for the same number of population doublings so that the switching frequencies in different strains could be compared fairly. We identified potential switchers by their resistance to ganciclovir (GCV) due to loss of TK transcription and confirmed that they no longer expressed the originally active VSG2 by dot blot analysis (Materials and Methods). The final VSG switching frequencies were normalized against the plating efficiencies determined for all strains (Supplementary Figure S2E).

The VSG switching frequency in *Tb*RAP1-depleted cells was increased 6.1–6.7-fold when compared to that in S/ev cells, while S and the uninduced S/RAP1i cells have similar switching frequencies to S/ev cells (Figure 1D). To confirm that the elevated switching frequency was specifically due to the lack of *Tb*RAP1, we introduced an inducible FLAG-HA-HA (F2H)-tagged *Tb*RAP1 expression vector into S/RAP1i cells. Adding doxycycline to S/RAP1i+F2H-*Tb*RAP1 cells induced F2H-*Tb*RAP1 expression (Supplementary Figure S2F) and resulted in a nearly normal growth (Supplementary Figure S2G) and a switching frequency comparable to that in S/ev cells (Figure 1D), indicating that expression of the ectopic F2H-*Tb*RAP1 suppressed the abnormal switching phenotype caused by *Tb*RAP1 depletion. Therefore, *Tb*RAP1 suppresses VSG switching.

VSG gene conversion is the most frequent switching events in *Tb*RAP1-depleted cells

By examining the genotype (detecting the presence of the *VSG2* and *BSD* genes by PCR, Supplementary Figure S3A and B) and marker expression status in recovered VSG switchers, we determined the switching mechanism in each switcher (Supplementary Figure S1; Tables S1–S6) (21). In S, S/ev, and uninduced S/RAP1i cells, most switchers (68-78%) arose from ES GC or ES Loss coupled with an *In Situ* (ESLIS) switch, and 16–32% of the switchers arose from VSG GC (Figure 1D, Supplementary Table S1–S3). However, in *Tb*RAP1-depleted cells, most switchers arose from VSG GC (62–74%), while fewer switchers arose through ES GC or ESLIS (19–26%) (Figure 1D, Supplementary Tables S5 and S6). The portion of cells that switched through an *in situ* or a CO/TE did not seem to change significantly upon *Tb*RAP1 depletion (Figure 1D). When the ectopic F2H-*Tb*RAP1 was expressed in S/RAP1i, ES GC or ESLIS were again the most frequent events (50%) and fewer cells switched through VSG GC (43%) (Figure 1D; Supplementary Table S4).

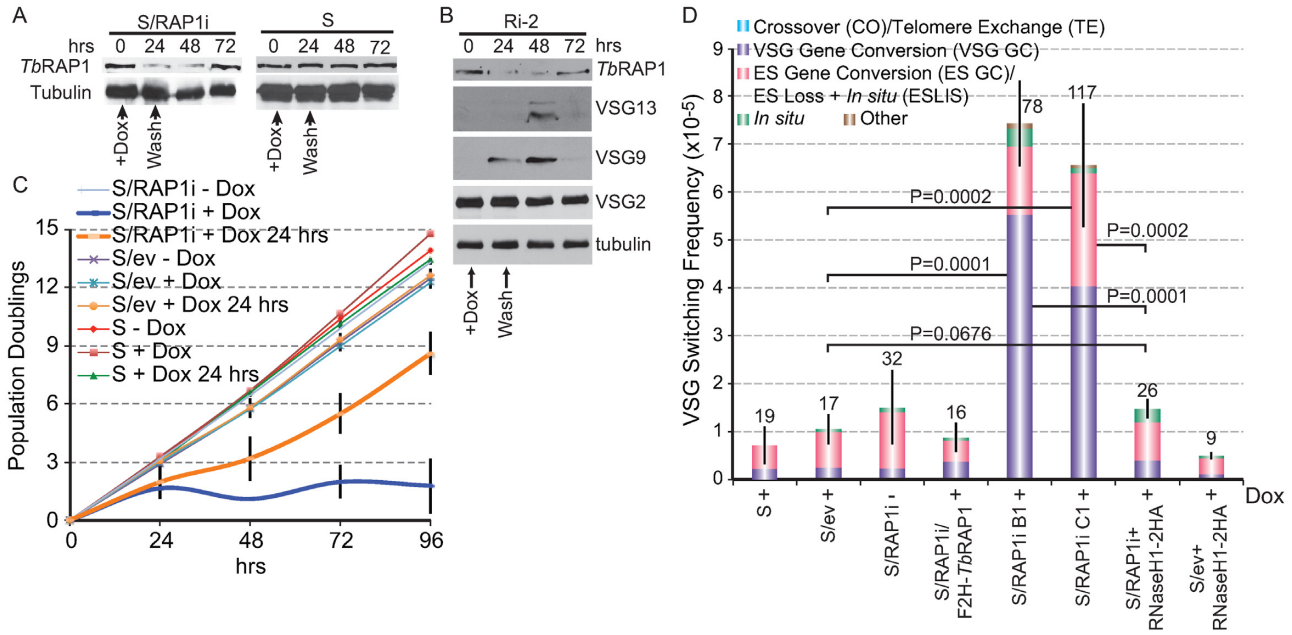

Figure 1. A transient depletion of *Tb*RAP1 increased VSG switching frequency. Western analyses of protein levels of *Tb*RAP1 and tubulin in S/RAP1i and S cells (**A**) and various ES-linked VSGs in Ri-2 (*Tb*RAP1 RNAi) cells (15) (**B**) at different time points. For transient induction, doxycycline was only added for 24 h. Cells used in (A) and (B) are VSG2-expressors. (**C**) Growth curves of S, S/ev, and S/RAP1i cells under induced (+Dox), uninduced (−Dox), and transiently induced (+Dox for 24 h) conditions. Average population doublings were calculated from three independent experiments. (**D**) VSG switching frequencies in S, S/ev, S/RAP1i, S/RAP1i+F2H-*Tb*RAP1, S/RAP1i+RNaseH1-2HA, and S/ev+RNaseH1-2HA cells with (+) or without (−) a transient induction are shown. B1 and C1 are independent clones of S/RAP1i. Average switching frequencies were calculated from at least four independent assays. *P* values (unpaired *t* tests) are indicated. The full height of each column represents 100% of analyzed switching events in the corresponding strain (total number of analyzed switchers is shown). Percentages of different VSG switching events are represented by heights of different colored bars. In (C) and (D), standard deviations are shown as error bars.

To confirm that we classified switchers correctly, we randomly selected switchers derived from induced S/RAP1i cells and analyzed their karyotypes. We first determined which VSGs were expressed in the recovered switchers by RT-PCR and sequencing analysis (Materials and Methods). Subsequently, undigested genomic DNA isolated from these switchers were separated by Pulsed-Field Gel Electrophoresis (PFGE) and analyzed by Southern blotting using the *BSD*, the originally active *VSG2*, and the newly active *VSG* probes. For all randomly selected switchers, their predicted VSG switching mechanisms were confirmed by karyotype analysis (Supplementary Figure S3C–E). Interestingly, karyotype analysis showed that all analyzed switchers that could have arisen from an ES GC or an ESLIS turned out to be the latter type. Although we cannot perform the extremely laborious karyotype studies for all switchers, this observation, based on a random sample, suggests that ESLIS is preferred to ES GC in S/RAP1i cells.

Depletion of *Tb*RAP1 leads to more DSBs at telomeres and subtelomeres

Removal of *Tb*RAP1 led to more VSG GC, which frequently initiates with DSBs. Therefore, we anticipated that depletion of *Tb*RAP1 might increase DSBs at telomeres and subtelomeres. RAD51 is a recombinase that binds to the single stranded 3′ overhang after 5′ end resection at DSB sites and mediates strand invasion during homologous recombination (38), and *Tb*RAD51 associates with the chromatin at break sites (17,18). Similarly, the C-terminally phosphorylated histone H2A (γH2A) is deposited at DNA break sites (39). Therefore, we performed Chromatin IP (ChIP) using the *Tb*RAD51 antibody (18) and a γH2A-specific antibody (see below) followed by Southern slot blotting and quantitative PCR (qPCR) in S/RAP1i cells.

We raised rabbit antibodies that specifically recognize γH2A or unphosphorylated H2A (Materials and Methods). After treating WT cells with 1.5 μg/ml phleomycin that induces DSBs (39), we detected γH2A by western blotting (Supplementary Figure S4A), confirming the specificity of the γH2A antibody (Supplementary Figure S4A).

We performed ChIP using *Tb*RAD51 and γH2A antibodies. Normal rabbit IgG was used as a negative control. The ChIP products were first analyzed by Southern slot blotting using a telomeric probe (Figure 2A and Supplementary Figure S4B) and, as a control, a probe specific to the 50 bp repeats that are located upstream of ES promoters (Supplementary Figure S4B and C). Upon depletion of *Tb*RAP1, more *Tb*RAD51 and γH2A were associated with the telomeric chromatin (Figure 2A) but not with the 50 bp repeats (Supplementary Figure S4C). In S/ev cells, adding doxycycline did not change the amount of telomere- or 50 bp repeats-associated *Tb*RAD51 or γH2A (Figure 2A, Supplementary Figures S4B and S4C). These observations suggest more DNA damage at the telomere upon *Tb*RAP1 depletion.

We also analyzed the ChIP products by qPCR using primers specific to *VSG2* (active), *VSG21* (ES-linked, silent), and ES promoters (one active and multiple silent),

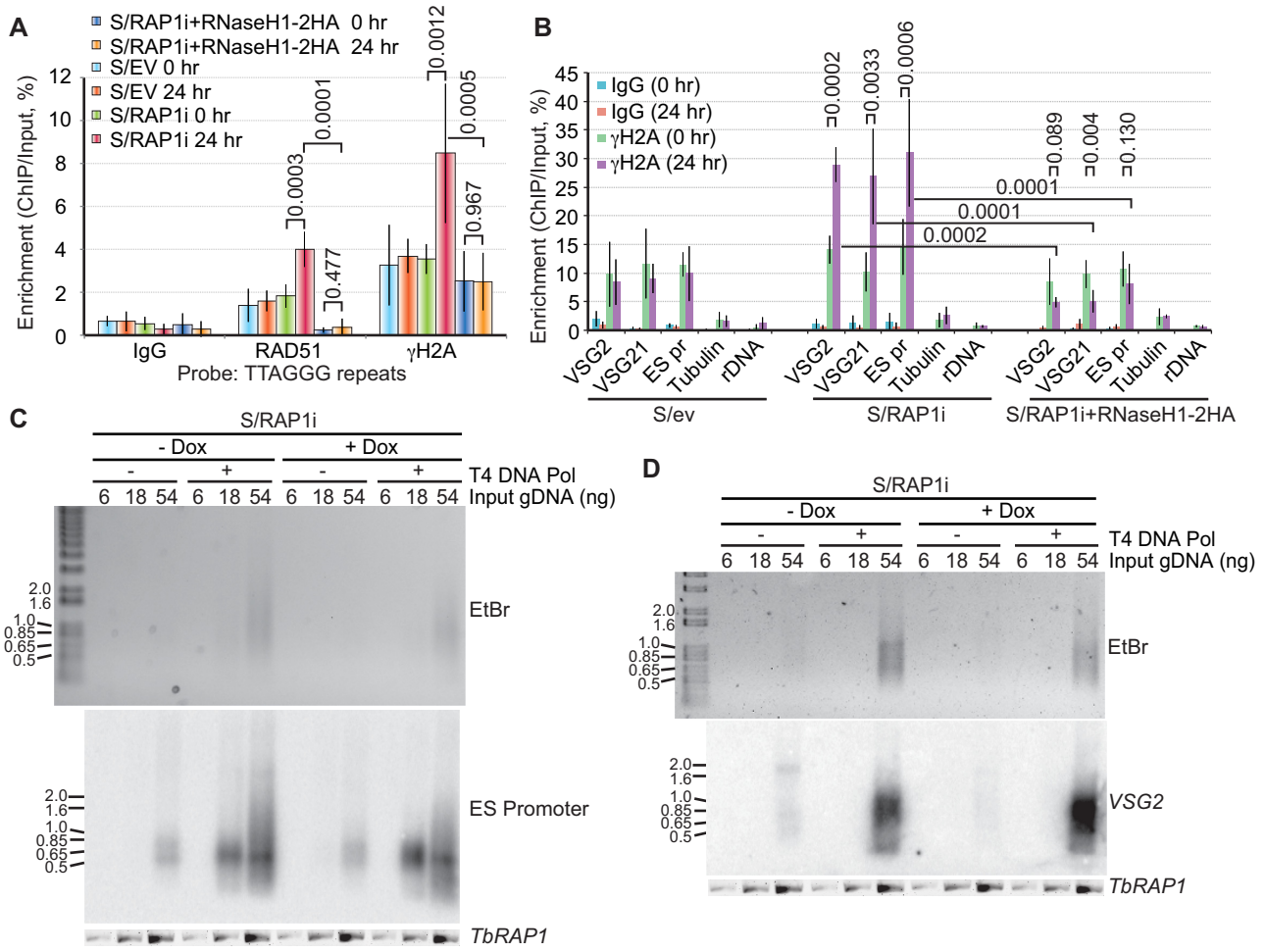

Figure 2. Depletion of *Tb*RAP1 resulted in more telomeric/subtelomeric DSBs. (**A**) ChIP experiments were performed using rabbit antibodies recognizing *Tb*RAD51 (18), γH2A, or normal rabbit IgG (as a negative control) in S/ev, S/RAP1i, and S/RAP1i+RNaseH1-2HA cells before (0 h) and after adding doxycycline (24 h). DNA isolated from ChIP products were hybridized with a TTAGGG repeat probe and exposed to a phosphorimager. The hybridization signals were quantified and averages were calculated from at least three independent experiments. (**B**) DNA isolated from ChIP experiments was analyzed by quantitative PCR (qPCR) using primers specific to *VSG2* (active), *VSG21* (silent), ES promoters, tubulin, and rDNA. Average enrichment (ChIP/input) was calculated from 3 to 12 independent experiments. In both (A) and (B), standard deviations are shown as error bars. *P* values of unpaired t-tests are shown. (**C** and **D**) LMPCR analyses were performed in S/RAP1i cells. The LMPCR products were hybridized with ES promoter (C) and *VSG2* (D) probes: the Ethidium bromide (EtBr)-stained LMPCR products are shown at the top, the Southern blot result is shown in the middle, and the PCR products using primers specific to the *TbRAP1* gene (as a loading control) are shown at the bottom. The amounts of input genomic DNA, from uninduced (−Dox) or induced (+Dox) cells, either treated (+) or untreated (−) with T4 DNA polymerase, are marked on top of each lane.

tubulin, and rDNA. As shown in Figure 2B and Supplementary Figure S4D, we observed a significant increase in the amount of ES-associated *Tb*RAD51 and γH2A upon depletion of *Tb*RAP1, suggesting that depletion of *Tb*RAP1 resulted in more DNA damage at ESs. No significant change was observed in S/ev cells before and after adding doxycycline.

Although association of *Tb*RAD51 and γH2A with the chromatin strongly suggests that DSBs occurred at the examined loci, ChIP results are still an indirect evidence for DSBs. We therefore performed Ligation-Mediated PCR (LMPCR; Supplementary Figure S5A) and examined ES regions for DSBs before and after depletion of *Tb*RAP1. LMPCR detects DSBs physically (40,41), although it cannot be used to detect DSBs at telomeres quantitatively due to the repetitive sequence. Interestingly, we detected more LMPCR products upon *Tb*RAP1 depletion when ES-linked *VSG* probes were used, including the active *VSG2* (Figure 2D) and derepressed *VSG15* (Supplementary Figure S5B) and *VSG21* (Supplementary Figure S5C), and this increase was significant (Supplementary Figure S5G). However, no increase in LMPCR products were seen when ES promoter (Figure 2C) or the 70 bp repeat probes (Supplementary Figure S5D) were used. We did not detect any change in DSB levels at *VSG* loci in S/ev cells (Supplementary Figure S5F). Depletion of *Tb*RAP1 did not increase the number of DSBs at a random chromosome internal *SNAP50* locus (Supplementary Figure S5E), indicating that the effect of *Tb*RAP1 depletion is telomere/subtelomere-specific.

It is worth to note that even in WT cells DSBs are detected in ESs, which is the same as demonstrated previously (42). Therefore, *Tb*RAP1 does not suppress subtelomeric DSBs completely. Additionally, in uninduced S/RAP1i

cells, a significant amount of LMPCR products of ∼2 kb was detected without T4 DNA polymerase treatment, indicating that these DSBs are blunt-ended and are located downstream of the active *VSG2*, as the *VSG2* gene is 1.43 kb (Figure 2D). Previously, it has been shown that DSBs downstream of the active *VSG* lead to more ES GC/ESLIS, while DSBs immediately upstream of the active *VSG* result in mostly VSG GC (3). Therefore, having DSBs downstream of the active *VSG2* is likely the reason that ES GC/ESLIS switchers are the most popular in WT cells. In contrast, in *Tb*RAP1-depleted cells, blunt-ended DSBs are rare and nearly all LMPCR products are of ∼700 bp, indicating that these DSBs are located within the *VSG2* gene. Since VSG is essential (43) and gene conversion often initiates with DSBs, it is likely that VSG GC is the most efficient repair mechanism to allow cells recover from this detrimental damage, which would explain why VSG GC switchers are predominant in *Tb*RAP1-depleted cells.

The active ES-adjacent telomere is transcribed

To investigate why depletion of *Tb*RAP1 caused more DSBs at telomeres and subtelomeres, we examined other phenotypes and found that *Tb*RAP1 suppresses telomere transcription (see below).

In *T. brucei*, a long, non-coding RNA containing the 5′ UUAGGG 3′ repeat sequence was identified previously (29). This transcript was not affected by 1 mg/ml α-Amanitin, suggesting that it was transcribed by RNAP I (29). However, where this RNA was transcribed from was unknown. We first performed northern analysis to detect the telomeric transcript. Total RNA was extracted from WT bloodstream form cells and treated with excessive amount of RNase-free DNase I. RNA samples were then hybridized with a $(CCCTAA)_n$ telomeric probe (Figure 3A, left), a $(TTAGGG)_n$ telomeric probe (Figure 3A, right), or a *Tb*TR probe (as a loading control, Figure 3A). We only detected the telomeric transcript (hereafter referred to as TERRA) when the $(CCCTAA)_n$ probe was used (Figure 3A), confirming that TERRA has a G-rich sequence. TERRA sizes range from a few hundred to ∼4k nucleotides in WT cells (Figure 3A). As a control, an equal amount of RNA was treated with RNase One and RNase A, which abolished the hybridization signal (Figure 3A).

It was hypothesized that TERRA was a product of RNAP I read-through from the active ES into the downstream telomeric repeats (29), although this was not proved. Because ES genes are polycistronically transcribed and trans-spliced, we reason that there must be some nascent RNA molecules containing both telomeric repeats and the upstream *VSG* sequence if TERRA is a read-through product from the active ES. We performed an RT-PCR experiment to test this possibility. In cells that express VSG2, total RNA was isolated and RT was performed using a TELC20 (5′-CCCTAACCCTAACCCTAACC-3′), a TELG20 (5′-GGGTTAGGGTTAGGGTAAGG-3′), or a random hexamer as the primer. An RT without any primer was also performed as a negative control. Subsequently, the RT products were amplified by PCR using primers specific to *VSG2* (active), *VSG9* (silent), 70 bp repeats, rRNA, and tubulin. We found that TELG20-primed RT products did not yield any PCR products using any primer pairs (Figure 3B), while the TELC20-primed RT products yielded a PCR product only when *VSG2*-specific primers were used (Figure 3B). As a positive control, all actively transcribed genes (including *VSG2*, rRNA and tubulin) gave a positive PCR product when a random hexamer was used in RT (Figure 3B). As expected, when RT was done without any primer, no PCR products were observed. This result indicates that TERRA is UG-rich, and *VSG2* (but not *VSG9*) and TERRA are co-transcribed, confirming the hypothesis that TERRA is transcribed from the active ES-adjacent telomere.

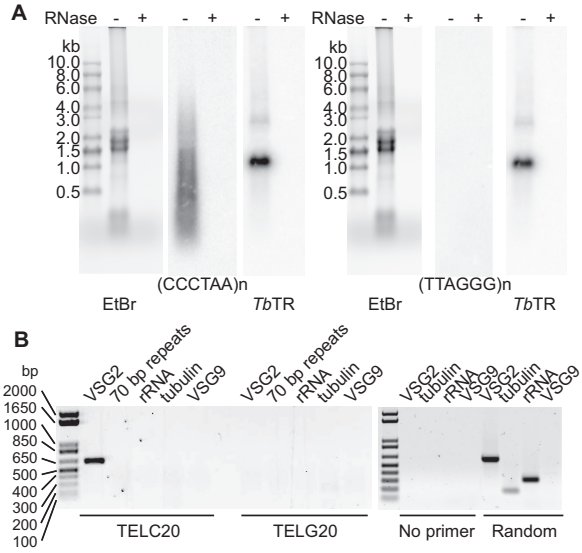

Figure 3. The active VSG-adjacent telomere was transcribed into TERRA. (**A**) Northern analysis of RNA isolated from WT cells. The northern blot was hybridized with a $(CCCTAA)_n$ probe (left panel) or a $(TTAGGG)_n$ probe (right panel). In each panel, the EtBr-stained gel (left), the TTAGGG/CCCTAA hybridization result (middle), and the hybridization result using a *Tb*TR (50) probe (right, as a loading control) are shown. Both RNA samples treated with or without RNase One and RNase A (RNase) were run. (**B**) Total RNA was purified from VSG2-expressing WT cells and reverse-transcribed using TELC20, TELG20, a random hexamer (as a positive control), or ddH_2O (as a negative control) as the RT primer (labeled beneath each gel). The RT products were PCR amplified using primers specific to *VSG2* (active), *VSG9* (silent), 70 bp repeats, tubulin and rRNA (marked on top of each lane), and the PCR products were separated on agarose gels.

To further validate our conclusion, we performed the same RT-PCR in a VSG9-expressor (where VSG2 and VSG3 are silent, Supplementary Figure S6A) and a VSG3-expressor (where VSG8 and VSG9 are silent while the *VSG2* gene is lost, Supplementary Figure S6B) (15) and obtained similar results: The TELC20-primed RT products were amplified only when the primers specific to the active *VSG* were used in PCR (Supplementary Figure S6). Therefore, TERRA is transcribed from the active ES-adjacent telomere but not from silent ES-adjacent telomeres.

Depletion of *Tb*RAP1 increases the TERRA level

Because depletion of *Tb*RAP1 derepresses subtelomeric *VSGs* (Figure 1B) (15,16), we hypothesize that *Tb*RAP1 also regulates TERRA expression.

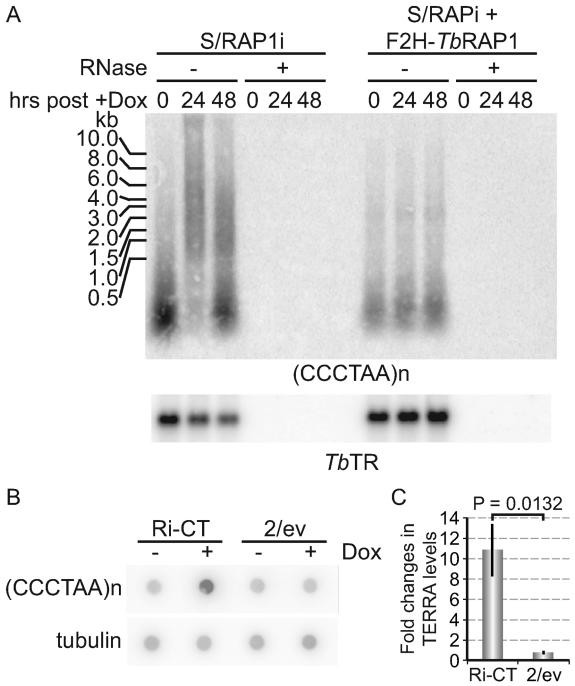

Figure 4. Depletion of *Tb*RAP1 increased the TERRA level. (**A**) Northern analysis of TERRA [hybridized with the (CCCTAA)n probe] in S/RAP1i and S/RAP1i+F2H-*Tb*RAP1 cells before (0 h) and after adding doxycycline (24 and 48 h). The *Tb*TR hybridization was used as a loading control. (**B**) Dot blot northern analysis of TERRA in Ri-CT (16) and 2/ev cells before and after adding doxycycline using a $(CCCTAA)_n$ and a tubulin probe. (**C**) Quantification of dot blot hybridization. Fold changes in TERRA RNA and tubulin mRNA signal intensities between 0 and 24 h after adding doxycycline were calculated from three independent experiments. Standard deviations are shown as error bars. *P* values of unpaired t-test are shown.

We first examined TERRA in S/RAP1i cells by northern blotting as described above. When *Tb*RAP1 was depleted, we observed stronger hybridization signals of much larger sizes (up to ∼10 kb) (Figure 4A). However, in S/RAP1i+F2H-*Tb*RAP1 cells, the level and size of TERRA remained unchanged before and after adding doxycycline (Figure 4A).

We also performed northern slot blot analysis to better quantify the amount of TERRA in *Tb*RAP1-depleted cells. In a previously established *Tb*RAP1 RNAi strain [Ri-CT, (16)] and the control strain carrying an empty RNAi vector (2/ev), total RNAs were isolated and slot-blotted onto a nylon membrane, then hybridized with the $(CCCTAA)_n$ probe and a tubulin probe (as a loading control) (Figure 4B). Quantification of the hybridization signals from three independent inductions indicated that the TERRA level in *Tb*RAP1-depleted cells was ∼11-fold of that in uninduced cells (Figure 4C). The TERRA level was not changed in 2/ev cells before and after adding doxycycline (Figure 4C). Therefore, loss of *Tb*RAP1 leads to an increase in the TERRA level.

Depletion of *Tb*RAP1 results in derepression of silent ESs (15,16). Therefore, we hypothesize that TERRA is expressed from the derepressed ES-adjacent telomeres in addition to the fully active telomere upon *Tb*RAP1 depletion. To test this, we performed the same RT-PCR experiment described above. In uninduced S/RAP1i cells, only primers specific to the active *VSG2* yielded a PCR product with the cDNA generated from the TELC20-primed RT reaction (Figure 5A), indicating that TERRA was transcribed from the active *VSG2*-adjacent telomere but not from silent *VSG3* or *VSG9*-adjacent telomeres. As expected, RT using TELG20 or no primer did not yield any PCR products (Figure 5A), and RT using the random hexamer yielded positive PCR products for active genes including *VSG2*, tubulin and rDNA (Figure 5A).

After *Tb*RAP1 RNAi was induced for 24 h, we were able to obtain PCR products for all active (*VSG2*, tubulin and rDNA) and derepressed (*VSG3*, *VSG9* and even 70 bp repeats) genes when the random hexamer was used in RT (Figure 5B), indicating that depletion of *Tb*RAP1 was successful. Surprisingly, when TELC20 was used as the RT primer, a positive PCR product was only obtained with VSG2 primers but not with VSG3 or VSG9 primers (Figure 5B). Therefore, even though depletion of *Tb*RAP1 results in derepression of ES-linked *VSGs* and increases the TERRA level, TERRA is still mainly expressed from the active *VSG*-adjacent telomere but little from derepressed *VSG*-adjacent telomeres, if any.

Depletion of *Tb*RAP1 leads to an increased amount of telomeric RNA:DNA hybrids

In human and yeast cells, TERRA has been shown to form RNA:DNA hybrids with the telomeric DNA, which presumably form a telomeric R-loop structure. R-loops increase DSB formation and thereby promote DNA recombination (30). Because a transient depletion of *Tb*RAP1 leads to increased VSG GC events at subtelomeres and increased TERRA level, we were curious whether *Tb*RAP1 depletion would also increase the number of telomeric RNA:DNA hybrids.

The S9.6 monoclonal antibody specifically recognizes the RNA:DNA hybrid (44) and has been routinely used to examine R-loops (34). We used S9.6 to immunoprecipitate (IP) all RNA:DNA hybrids from S/RAP1i cells before and after induction of *Tb*RAP1 RNAi. The IP products were then analyzed by dot blot hybridization using the $(TTAGGG)_n$ probe. We observed an increased telomeric RNA:DNA hybrid signal in *Tb*RAP1-depleted cells (Figure 6A). Treating genomic DNA with RNaseH (Thermo Fisher Scientific) before S9.6 IP reduced the precipitated telomeric signals to the background level, confirming that the detected signals are from an RNA:DNA hybrid structure. Quantification of the hybridization signals indicates that the amount of telomeric RNA:DNA hybrids in S/RAP1i cells increased nearly seventeen fold after induction of *Tb*RAP1 RNAi (Figure 6B). Therefore, depletion of *Tb*RAP1 results in many more telomeric RNA:DNA hybrids.

To determine whether the highly transcribed active VSG mRNA and the derepressed VSG mRNA in *Tb*RAP1-depleted cells also form an R-loop structure, we performed the same S9.6 IP followed by qPCR using primers specific to different *VSG* genes. However, we did not detect any VSG sequence-containing RNA:DNA hybrids in S/RAP1i cells before or after induction of RNAi, indicating that

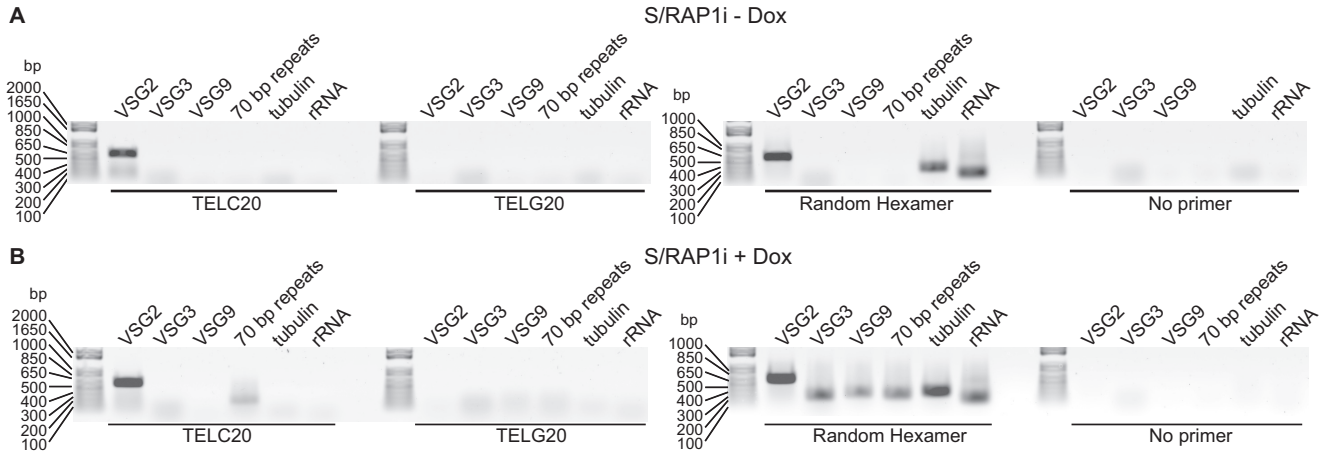

Figure 5. The active VSG-adjacent telomere was transcribed in *Tb*RAP1-depleted cells. The same RT-PCR experiment as described in Figure 3B was performed in S/RAP1i cells before (**A**) and after (**B**) induction of *Tb*RAP1 RNAi. RT primers were listed below each gel, while primers used in PCR amplification were listed on top of each lane.

the amount of RNA:DNA hybrids formed with the VSG mRNA, if any, is extremely low.

Expressing an ectopic WT allele of *Tb*RNaseH1 in *Tb*RAP1 RNAi cells reduces the telomeric RNA:DNA hybrids back to WT levels

RNA:DNA hybrids can be resolved by RNaseH, which cleaves the RNA strand in the RNA:DNA hybrid (35). In *T. brucei*, *Tb*RNaseH1 (*Tb*427.07.4930) was characterized previously (45). We therefore cloned a C-terminally HA-HA (2HA) tagged *Tb*RNaseH1 into an inducible expression vector, pLew100v5 (13), and transfected it into S/RAP1i and S/ev (as a control) cells. In S/ev+RNaseH1-2HA cells, *Tb*RNaseH1-2HA was only expressed upon adding doxycycline (Supplementary Figure S7A). In S/RAP1i+RNaseH1-2HA, however, there was a low level leaky expression of *Tb*RNaseH1 before adding doxycycline, which was induced to a higher level upon addition of doxycycline (Supplementary Figure S7A). Importantly, adding doxycycline in these cells also induced *Tb*RAP1 depletion by RNAi (Supplementary Figure S7A). In addition, we observed derepression of previously silent VSGs, including VSG 3, 8, 13, 18 and mVSG397 (Supplementary Figure S7B), confirming that expression of an ectopic *Tb*RNaseH1 does not suppress the VSG-derepression phenotype in *Tb*RAP1-depleted cells.

Subsequently, we performed S9.6 IP using genomic DNA isolated from S/RAP1i+RNaseH1-2HA cells followed by Southern slot blotting. As expected, the amount of telomeric RNA:DNA hybrid was approximately the same before and after induction, unlike what we observed in S/RAP1i cells (Figure 6). Clearly, expressing an ectopic allele of *Tb*RNaseH1 in S/RAP1i cells suppressed the phenotype of more telomeric RNA:DNA hybrids.

Because silent VSGs were derepressed in S/RAP1i+RNaseH1-2HA cells upon adding doxycycline (Supplementary Figure S7B), we did not expect that expression of *Tb*RNaseH1 would affect TERRA expression. Northern analysis using the C-rich telomeric probe showed that although the TERRA level in induced S/RAP1i+RNaseH1-2HA cells was lower than that in induced S/RAP1i cells, it was still significantly higher than that in WT cells (Supplementary Figure S7C and D). RNaseH1 degrades the RNA strand in the RNA:DNA hybrids (35), which is presumably the reason why less TERRA was detected when an ectopic allele of *Tb*RNaseH1 was expressed.

Expressing an ectopic allele of *Tb*RNaseH1 in *Tb*RAP1 RNAi cells suppresses the phenotype of more DSBs at telomeres/subtelomeres and that of elevated VSG switching frequency

We hypothesize that more telomeric RNA:DNA hybrids is the reason for increased amount of telomeric/subtelomeric DSBs in *Tb*RAP1-depleted cells. To test this, we examined the association of *Tb*RAD51 and γH2A with the telomeric/subtelomeric chromatin by ChIP in S/RAP1i+RNaseH1-2HA cells. In contrast to S/RAP1i cells, adding doxycycline to S/RAP1i+RNaseH1-2HA cells did not increase the association of *Tb*RAD51 or γH2A with the telomeric (Figure 2A and Supplementary Figure S4B) or ES (Figure 2B and Supplementary Figure S4D) chromatin.

We also hypothesize that more VSG switching events in *Tb*RAP1-depleted cells are due to more telomeric/subtelomeric DSBs. To test this, we performed an *in vitro* VSG switching analysis in S/RAP1i+RNaseH1-2HA cells. Strikingly, the switching frequency in transiently induced S/RAP1i+RNaseH1-2HA cells was very similar to that in S/ev cells (Figure 1D). Furthermore, most switchers arose from ES GC or ESLIS (54%, Supplementary Table S7), which was the same as that in WT cells (Figure 1D). Ectopic expression of *Tb*RNaseH1 in S/ev cells resulted in a VSG switching frequency comparable to that in S cells (Figure 1D, Supplementary Table S8). Therefore, expressing an ectopic allele of *Tb*RNaseH1 in *Tb*RAP1-depleted cells reduced telomeric RNA:DNA

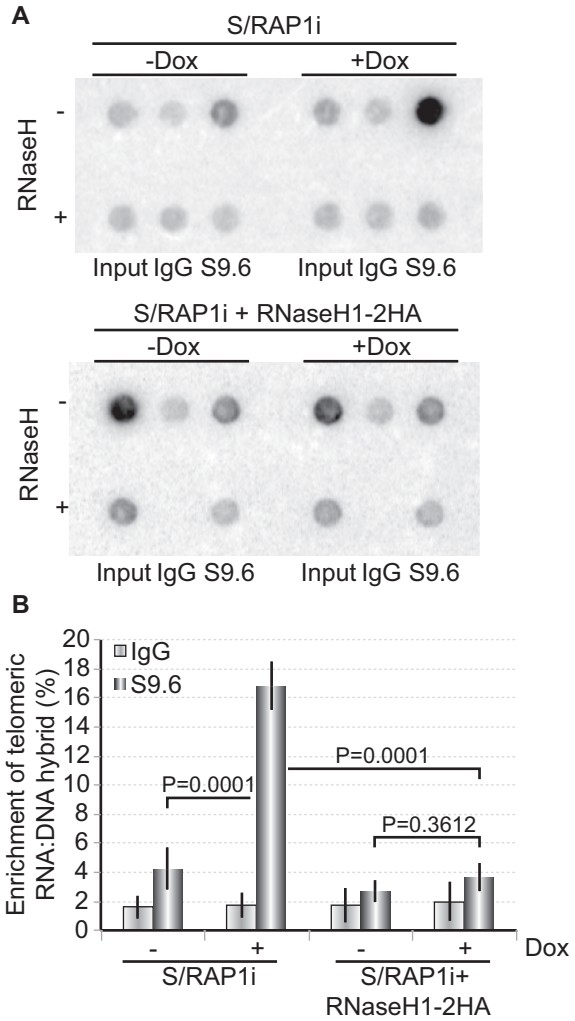

Figure 6. Depletion of *Tb*RAP1 led to increased amount of telomeric RNA:DNA hybrids, which was suppressed by ectopic expression of *Tb*RNaseH1. (**A**) Dot blot Southern analysis of input (diluted 20-fold), IgG and S9.6 immunoprecipitated DNA samples in S/RAP1i cells (top) and S/RAP1i+RNaseH1-2HA cells (bottom) before (–Dox) and after (+Dox) adding doxycycline for 24 h. Samples were treated with or without RNaseH (Thermo Fisher Scientific) before IP. A $(TTAGGG)_n$ probe was used in the hybridization. (**B**) Quantification of the dot blot hybridization signals. Average values were calculated from at least four independent experiments. Standard deviations are shown as error bars. Unpaired *t*-test *P* values are indicated.

hybrids, telomeric/subtelomeric DSBs, and VSG switching frequency to WT levels.

DISCUSSION

*Tb*RAP1 is essential for cell proliferation (15), but the reason was unknown. Now we show that lack of *Tb*RAP1 leads to more DSBs at the telomere and ES-linked *VSG* loci. Since introducing a DSB near the active *VSG* results in >90% of cell death (3), increased telomeric/subtelomeric DSBs would be an important factor for growth arrest in *Tb*RAP1-depleted cells. Interestingly, *Tb*RAP1's function in maintaining telomere and subtelomere integrity is linked with its role in telomeric silencing, because *Tb*RAP1-

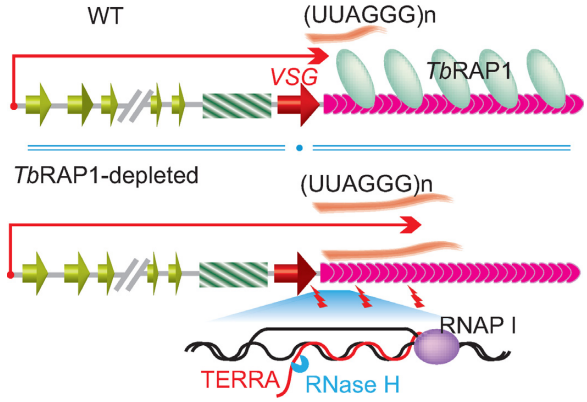

Figure 7. *Tb*RAP1 suppresses VSG switching by repressing TERRA and telomeric RNA:DNA hybrids. We hypothesize that the presence of *Tb*RAP1 at the telomere (top) helps blocking excessive read-through of RNAP I into the telomeric repeats from the active ES. Removal of *Tb*RAP1 from the telomere (bottom) may allow RNAP I to travel longer along the telomere and yield a higher TERRA level (orange strips), which leads to increased amount of telomeric RNA:DNA hybrids (magnified below the blue shade) and subsequent DNA damage (red bolts) at the subtelomere/telomere vicinity. The telomere complex is extremely simplified in the diagram. Alternative hypotheses are discussed in the text.

depletion results in an increased TERRA level and more telomeric RNA:DNA hybrids that in turn promote more DSBs at telomeres and subtelomeres, which are a potent trigger for VSG switching (Figure 7) (42). This is different from the protective roles of *Tb*TRF and *Tb*TIF2, two other telomere proteins that are important for maintaining subtelomere stability (24,25,27,37). Neither *Tb*TRF nor *Tb*TIF2 is required for VSG silencing (15,25). Depletion of *Tb*TRF or *Tb*TIF2 led to different subtelomeric DNA damage profiles than depletion of *Tb*RAP1 (25,27). Therefore, although all known *T. brucei* telomere proteins, when depleted, result in more switchers, the underlying mechanisms are different.

A previous study strongly suggests that *T. brucei* TERRA is transcribed by RNAP I (29). We have confirmed that the active *VSG*-adjacent telomere is transcribed while telomeres adjacent to silent ESs are not, which is consistent with the hypothesis that TERRA results from read-through of the active ES by RNAP I. However, we do not know whether telomeres that do not harbor any ESs are transcribed. A ribosomal RNA promoter has been found at a minichromosome subtelomere (46), and it may transcribe the downstream telomere.

Depletion of *Tb*RAP1 increases the TERRA level, but TERRA is still mainly transcribed from the active ES-adjacent telomere. Since the derepressed ESs are transcribed at a level that is still 10–100-fold lower than the active ES (16), read-through of the derepressed ESs may be too low to be detected. This is also consistent with our previous observation that loss of *Tb*RAP1 did not affect ES chromatin structure significantly in bloodstream form *T. brucei* cells (16). The active ES expression is not increased by the loss of *Tb*RAP1 (15). Additionally, no dramatic telomere length change has been detected when *Tb*RAP1 was depleted for two days (15). Therefore, longer TERRA species in *Tb*RAP1-depleted cells suggests that removal of

*Tb*RAP1 allows RNAP I to travel longer along the telomere downstream of the active ES (Figure 7). In *Tb*RAP1-depleted cells, the TELC20-primed RT product yielded a low level of PCR product using primers specific to 70 bp repeats (Figure 5B), suggesting that some RNA molecules contain both telomeric and 70 bp repeat sequences. Hence, lacking *Tb*RAP1 may also affect TERRA RNA processing and allow accumulation of more unprocessed TERRA and telomeric RNA:DNA hybrids (see below). Further studies are necessary to elucidate exactly how *Tb*RAP1 regulates TERRA expression.

R-loops are three-stranded structure formed by an RNA:DNA hybrid plus a displaced single-stranded DNA (47), which is sensitive to RNaseH (35) and can be recognized by the S9.6 antibody (44). Excessive R-loops cause genome instability, as R-loops can stall DNA replication and collapsed replication fork often results in DSBs (34,47). In addition, processing of R-loops by transcription-coupled nucleotide excision repair factors can induce DSBs (47). However, exactly how R-loops promote DSB formation is still unclear. TERRA can form the R-loop structure with the telomeric DNA in mammalian and yeast cells, which promotes telomere recombination (30). We detected more telomeric RNA:DNA hybrids and increased association of *Tb*RAD51 and γH2A with the telomere and subtelomere chromatin upon *Tb*RAP1 depletion, suggesting more DNA damage at telomeres/subtelomeres (which is confirmed by LMPCR) due to increased telomeric RNA:DNA hybrids, which is suppressed by ectopic expression of *Tb*RNaseH1. These observations support the model that excessive telomeric R-loops affect telomeric/subtelomeric integrity (Figure 7). So far, it is unclear exactly where R-loop-induced DSBs are located (47). However, we anticipate that telomeric R-loop induced DNA damage is concentrated at the telomere (Figure 7). In our strain, the distance from the end of each *VSG* gene to the first TTAGGG repeat is 0.7 kb (*VSG2*), 0.8 kb (*VSG15*) and 1.5 kb (*VSG21*), respectively (10). Therefore, it is reasonable that we detect more DSBs by LMPCR within or downstream of these *VSG* genes, as they are immediately adjacent to the telomere.

Depletion of *Tb*RAP1 increased TERRA level, which presumably leads to more telomeric RNA:DNA hybrids. However, it is possible that *Tb*RAP1 may also suppress the formation of the telomeric RNA:DNA hybrid or facilitates its resolution directly. Alternatively, it is possible that *Tb*RAP1 depletion affects telomeric DNA replication, which results in accumulation of RNA:DNA hybrids as a replication intermediate. Further investigation will be necessary to test these possibilities. TERRA is only transcribed from the active ES-adjacent telomere, but DSBs are detected downstream of both active and silent *VSGs*, suggesting that telomeric RNA:DNA hybrids are formed at both active and silent telomeres. Whether TERRA can function both in *cis* and in *trans* and pair with both active and silent telomeric DNA will need further investigation in the future.

LMPCR did not detect increased DSBs in 70 bp repeats or at ES promoters (which are a few kb or 40–60 kb upstream of the ES-linked *VSGs*, respectively) in *Tb*RAP1-depleted cells. However, more γH2A and *Tb*RAD51 were associated with the ES promoters and telomeres upon *Tb*RAP1 depletion. This discrepancy may be due to several reasons. First, LMPCR detects physical DSBs, but it is not efficient to detect breaks in repetitive sequences or if DSBs are located far from the place where the locus-specific primer anneals. Second, γH2A can spread more than tens of kilobases around the DSB in yeast (48), and it may spread equally far from the break in *T. brucei*. Third, RAD51 is important to keep genome integrity when DNA replication is stalled (49). ES replication may be affected by downstream telomeric RNA:DNA hybrids, which leads to accumulation of *Tb*RAD51 along the whole ES. Particularly, the active ES replicates early (20) and may be more sensitive to replication defects.

We did not detect any R-loops at the ES-linked *VSG* loci in either WT or *Tb*RAP1-depleted cells. In general, R-loops are rare in the genome. R-loops are often associated with high level of transcription, and G-clusters at the nontranscribed strand and negative superhelicity often facilitate R-loop formation (34). VSG sequences are apparently less G-rich than the telomeric repeats. In addition, efficient RNA processing appears to reduce the chance of R-loop formation (34). A large number of VSG proteins ($\sim 10^7$/cell) are synthesized, demanding a very efficient VSG mRNA processing. Therefore, VSG mRNAs are likely efficiently processed so that R-loops at *VSG* loci are extremely rare.

Many pathogens that undergo antigenic variation express their major surface antigens from subtelomeric regions, as subtelomere plasticity would facilitate antigen switching (2). Indeed, *T. brucei* subtelomeres are fragile (3), which presumably facilitates DNA recombination-mediated VSG switching (42). However, DSBs at subtelomeres, particularly within the active ES, are deleterious to *T. brucei* (3). Therefore, it is essential to balance the stability and plasticity at subtelomeres, which is a delicate task. In the *Tb*RAP1-depleted cells, it is detrimental to cell viability to have many DSBs at telomeres/subtelomeres, even though DSBs are a potent trigger for recombination-mediated VSG switching. In summary, our data not only demonstrate that *Tb*RAP1 affects VSG switching by maintaining telomere and subtelomere integrity and stability but also showed that *Tb*RAP1-mediated telomeric silencing is the underlying mechanism of how *Tb*RAP1 suppresses subtelomeric DNA recombination. Importantly, we showed that abnormally high levels of TERRA and telomeric RNA:DNA hybrids cause genome instability that leads to deleterious effects, further underlying the importance of appropriate regulation of the telomeric transcript and RNA:DNA hybrid by *Tb*RAP1. For the first time, our study demonstrated the involvement of a long, non-coding RNA in antigenic variation and the mechanistic link between telomeric silencing and telomere integrity through the regulation of telomere transcription by a conserved telomere protein.

SUPPLEMENTARY DATA

Supplementary Data are available at NAR Online.

ACKNOWLEDGEMENTS

We thank H. Kim and G.A.M. Cross for HSTB261 cells, VSG-specific antibodies and the pLew100-Cre-EP1 and pLew100v5 plasmids. We are grateful to S. Leppla for the

S9.6 antibody and to R. McCulloch for the *Tb*RAD51 antibody. M. Imam, A. Denisyuk, H. Schmolz and O. Prica are thanked for their help in purification and characterization of the H2A and γH2A antibodies. We greatly appreciate the comments and suggestions from V. Boerner, A. Severson and the Li lab members.

FUNDING

National Institutes of Health (NIH) [AI066095 to B.L.]; GRHD Center at CSU (in part). Funding for open access charge: NIH; Center for Gene Regulation in Health and Disease at Cleveland State University.
Conflict of interest statement. None declared.

REFERENCES

1. Barry,J.D., Ginger,M.L., Burton,P. and McCulloch,R. (2003) Why are parasite contingency genes often associated with telomeres? *Int. J. Parasitol.*, **33**, 29–45.
2. Li,B. (2012) Telomere components as potential therapeutic targets for treating microbial pathogen infections. *Front. Oncol.*, **2**, 156.
3. Glover,L., Alsford,S. and Horn,D. (2013) DNA break site at fragile subtelomeres determines probability and mechanism of antigenic variation in African trypanosomes. *PLoS Pathog.*, **9**, e1003260.
4. Richards,M., Coppee,F., Thomas,N., Belayew,A. and Upadhyaya,M. (2012) Facioscapulohumeral muscular dystrophy (FSHD): an enigma unravelled? *Hum. Genet.*, **131**, 325–340.
5. Wise,J.L., Crout,R.J., McNeil,D.W., Weyant,R.J., Marazita,M.L. and Wenger,S.L. (2009) Cryptic subtelomeric rearrangements and X chromosome mosaicism: a study of 565 apparently normal individuals with fluorescent *in situ* hybridization. *PLoS One*, **4**, e5855.
6. Riethman,H., Ambrosini,A. and Paul,S. (2005) Human subtelomere structure and variation. *Chromosome Res.*, **13**, 505–515.
7. Cross,G.A.M., Kim,H.S. and Wickstead,B. (2014) Capturing the variant surface glycoprotein repertoire (the VSGnome) of *Trypanosoma brucei* Lister 427. *Mol. Biochem. Parasitol.*, **195**, 59–73.
8. Gunzl,A., Bruderer,T., Laufer,G., Schimanski,B., Tu,L.C., Chung,H.M., Lee,P.T. and Lee,M.G. (2003) RNA polymerase I transcribes procyclin genes and variant surface glycoprotein gene expression sites in *Trypanosoma brucei*. *Eukaryot. Cell*, **2**, 542–551.
9. de Lange,T. and Borst,P. (1982) Genomic environment of the expression-linked extra copies of genes for surface antigens of *Trypanosoma brucei* resembles the end of a chromosome. *Nature*, **299**, 451–453.
10. Hertz-Fowler,C., Figueiredo,L.M., Quail,M.A., Becker,M., Jackson,A., Bason,N., Brooks,K., Churcher,C., Fahkro,S., Goodhead,I. *et al.* (2008) Telomeric expression sites are highly conserved in *Trypanosoma brucei*. *PLoS ONE*, **3**, e3527.
11. Gunzl,A., Kirkham,J.K., Nguyen,T.N., Badjatia,N. and Park,S.H. (2015) Mono-allelic VSG expression by RNA polymerase I in *Trypanosoma brucei*: Expression site control from both ends? *Gene*, **556**, 68–73.
12. Batram,C., Jones,N.G., Janzen,C.J., Markert,S.M. and Engstler,M. (2014) Expression site attenuation mechanistically links antigenic variation and development in *Trypanosoma brucei*. *Elife*, **3**, e02324.
13. Cestari,I. and Stuart,K. (2015) Inositol phosphate pathway controls transcription of telomeric expression sites in trypanosomes. *Proc. Natl. Acad. Sci. U.S.A.*, **112**, E2803–E2812.
14. Kassem,A., Pays,E. and Vanhamme,L. (2014) Transcription is initiated on silent variant surface glycoprotein expression sites despite monoallelic expression in *Trypanosoma brucei*. *Proc. Natl. Acad. Sci. U.S.A.*, **111**, 8943–8948.
15. Yang,X., Figueiredo,L.M., Espinal,A., Okubo,E. and Li,B. (2009) RAP1 is essential for silencing telomeric variant surface glycoprotein genes in *Trypanosoma brucei*. *Cell*, **137**, 99–109.
16. Pandya,U.M., Sandhu,R. and Li,B. (2013) Silencing subtelomeric VSGs by *Trypanosoma brucei* RAP1 at the insect stage involves chromatin structure changes. *Nucleic Acids Res.*, **41**, 7673–7682.
17. McCulloch,R. and Barry,J.D. (1999) A role for RAD51 and homologous recombination in *Trypanosoma brucei* antigenic variation. *Genes Dev.*, **13**, 2875–2888.
18. Proudfoot,C. and McCulloch,R. (2005) Distinct roles for two RAD51-related genes in *Trypanosoma brucei* antigenic variation. *Nucleic Acids Res.*, **33**, 6906–6919.
19. Hartley,C.L. and McCulloch,R. (2008) *Trypanosoma brucei* BRCA2 acts in antigenic variation and has undergone a recent expansion in BRC repeat number that is important during homologous recombination. *Mol. Microbiol.*, **68**, 1237–1251.
20. Devlin,R., Marques,C.A., Paape,D., Prorocic,M., Zurita-Leal,A.C., Campbell,S.J., Lapsley,C., Dickens,N. and McCulloch,R. (2016) Mapping replication dynamics in *Trypanosoma brucei* reveals a link with telomere transcription and antigenic variation. *Elife*, **5**, e12765.
21. Kim,H.S. and Cross,G.A.M. (2010) TOPO3alpha influences antigenic variation by monitoring expression-site-associated *VSG* switching in *Trypanosoma brucei*. *PLoS Pathog.*, **6**, e1000992.
22. Kim,H.S. and Cross,G.A.M. (2011) Identification of *Trypanosoma brucei* RMI1/BLAP75 homologue and its roles in antigenic variation. *PLoS One*, **6**, e25313.
23. Hovel-Miner,G.A., Boothroyd,C.E., Mugnier,M., Dreesen,O., Cross,G.A.M. and Papavasiliou,F.N. (2012) Telomere length affects the frequency and mechanism of antigenic variation in *Trypanosoma brucei*. *PLoS Pathog.*, **8**, e1002900.
24. Jehi,S.E., Li,X., Sandhu,R., Ye,F., Benmerzouga,I., Zhang,M., Zhao,Y. and Li,B. (2014) Suppression of subtelomeric VSG switching by *Trypanosoma brucei* TRF requires its TTAGGG repeat-binding activity. *Nucleic Acids Res.*, **42**, 12899–12911.
25. Jehi,S.E., Wu,F. and Li,B. (2014) *Trypanosoma brucei* TIF2 suppresses VSG switching by maintaining subtelomere integrity. *Cell Res.*, **24**, 870–885.
26. Stewart,J.A., Chaiken,M.F., Wang,F. and Price,C.M. (2012) Maintaining the end: Roles of telomere proteins in end-protection, telomere replication and length regulation. *Mutat. Res.*, **730**, 12–19.
27. Jehi,S.E., Nanavaty,V. and Li,B. (2016) *Trypanosoma brucei* TIF2 and TRF suppress VSG switching using overlapping and independent mechanisms. *PLoS One*, **11**, e0156746.
28. Ottaviani,A., Gilson,E. and Magdinier,F. (2008) Telomeric position effect: from the yeast paradigm to human pathologies? *Biochimie*, **90**, 93–107.
29. Rudenko,G. and Van der Ploeg,L.H. (1989) Transcription of telomere repeats in protozoa. *EMBO J.*, **8**, 2633–2638.
30. Cusanelli,E. and Chartrand,P. (2015) Telomeric repeat-containing RNA TERRA: a noncoding RNA connecting telomere biology to genome integrity. *Front Genet.*, **6**, 143.
31. Luke,B., Panza,A., Redon,S., Iglesias,N., Li,Z. and Lingner,J. (2008) The Rat1p 5′ to 3′ exonuclease degrades telomeric repeat-containing RNA and promotes telomere elongation in *Saccharomyces cerevisiae*. *Mol. Cell*, **32**, 465–477.
32. Schoeftner,S. and Blasco,M.A. (2008) Developmentally regulated transcription of mammalian telomeres by DNA-dependent RNA polymerase II. *Nat. Cell. Biol.*, **10**, 228–236.
33. Iglesias,N., Redon,S., Pfeiffer,V., Dees,M., Lingner,J. and Luke,B. (2011) Subtelomeric repetitive elements determine TERRA regulation by Rap1/Rif and Rap1/Sir complexes in yeast. *EMBO Rep.*, **12**, 587–593.
34. Aguilera,A. and Garcia-Muse,T. (2012) R loops: from transcription byproducts to threats to genome stability. *Mol. Cell*, **46**, 115–124.
35. Cerritelli,S.M. and Crouch,R.J. (2009) Ribonuclease H: the enzymes in eukaryotes. *FEBS J.*, **276**, 1494–1505.
36. Arora,R., Lee,Y., Wischnewski,H., Brun,C.M., Schwarz,T. and Azzalin,C.M. (2014) RNaseH1 regulates TERRA-telomeric DNA hybrids and telomere maintenance in ALT tumour cells. *Nat. Commun.*, **5**, 5220.
37. Li,B., Espinal,A. and Cross,G.A.M. (2005) Trypanosome telomeres are protected by a homologue of mammalian TRF2. *Mol. Cell. Biol.*, **25**, 5011–5021.
38. Karpenshif,Y. and Bernstein,K.A. (2012) From yeast to mammals: recent advances in genetic control of homologous recombination. *DNA Repair (Amst.)*, **11**, 781–788.
39. Glover,L. and Horn,D. (2012) Trypanosomal histone gammaH2A and the DNA damage response. *Mol. Biochem. Parasitol.*, **183**, 78–83.
40. Catalan,N., Selz,F., Imai,K., Revy,P., Fischer,A. and Durandy,A. (2003) The block in immunoglobulin class switch recombination

caused by activation-induced cytidine deaminase deficiency occurs prior to the generation of DNA double strand breaks in switch mu region. *J. Immunol.*, **171**, 2504–2509.
41. Rush,J.S., Fugmann,S.D. and Schatz,D.G. (2004) Staggered AID-dependent DNA double strand breaks are the predominant DNA lesions targeted to S mu in Ig class switch recombination. *Int. Immunol.*, **16**, 549–557.
42. Boothroyd,C.E., Dreesen,O., Leonova,T., Ly,K.I., Figueiredo,L.M., Cross,G.A.M. and Papavasiliou,F.N. (2009) A yeast-endonuclease-generated DNA break induces antigenic switching in *Trypanosoma brucei*. *Nature*, **459**, 278–281.
43. Smith,T.K., Vasileva,N., Gluenz,E., Terry,S., Portman,N., Kramer,S., Carrington,M., Michaeli,S., Gull,K. and Rudenko,G. (2009) Blocking variant surface glycoprotein synthesis in *Trypanosoma brucei* triggers a general arrest in translation initiation. *PLoS One*, **4**, e7532.
44. Boguslawski,S.J., Smith,D.E., Michalak,M.A., Mickelson,K.E., Yehle,C.O., Patterson,W.L. and Carrico,R.J. (1986) Characterization of monoclonal antibody to DNA.RNA and its application to immunodetection of hybrids. *J. Immunol. Methods*, **89**, 123–130.
45. Kobil,J.H. and Campbell,A.G. (2000) *Trypanosoma brucei* RNase HI requires its divergent spacer subdomain for enzymatic function and its conserved RNA binding motif for nuclear localization. *Mol. Biochem. Parasitol.*, **107**, 135–142.
46. Zomerdijk,J.C.B.M., Kieft,R. and Borst,P. (1992) A ribosomal RNA gene promoter at the telomere of a mini-chromosome in *Trypanosoma brucei*. *Nucleic Acids Res.*, **20**, 2725–2734.
47. Sollier,J. and Cimprich,K.A. (2015) Breaking bad: R-loops and genome integrity. *Trends Cell Biol.*, **25**, 514–522.
48. Fillingham,J., Keogh,M.C. and Krogan,N.J. (2006) GammaH2AX and its role in DNA double-strand break repair. *Biochem. Cell Biol.*, **84**, 568–577.
49. Godin,S.K., Sullivan,M.R. and Bernstein,K.A. (2016) Novel insights into RAD51 activity and regulation during homologous recombination and DNA replication. *Biochem. Cell Biol.*, **94**, 407–418.
50. Sandhu,R., Sanford,S., Basu,S., Park,M., Pandya,U.M., Li,B. and Chakrabarti,K. (2013) A trans-spliced telomerase RNA dictates telomere synthesis in *Trypanosoma brucei*. *Cell Res.*, **23**, 537–551.